ELSEVIER

Journal of Alloys and Compounds 260 (1997) 211–216

Journal of ALLOYS AND COMPOUNDS

Hydriding properties of Ce(Mn, Al)$_2$ and Ce(Fe, Al)$_2$ intermetallic compounds

P. Spatz*, K.J. Gross, A. Züttel, L. Schlapbach

Solid State Physics, University of Fribourg, Ch-1700 Fribourg, Switzerland

Received 14 March 1997

Abstract

A major breaktrough in the developement of metal hydrides for hydrogen storage will require inexpensive intermetallic compounds that absorb large quantities of hydrogen at near ambient conditions (atmospheric pressure and room temperature). Unfortunately, in the last ten years there has been relatively little progress in this field. We investigated intermetallic compounds Ce($T_{1-y}Al_y$)$_2$ with T=Mn, Fe in the range $0.5 \leq y < 1.0$. Mn, Fe and Al are inexpensive and Ce could be replaced by the low cost mischmetal (MM). The intermetallic compounds Ce(T, Al)$_2$ form the C14 and C15 Laves phases and they absorb hydrogen. A fraction of the totally absorbed hydrogen of about 2.5 H/(formula unit) forms a stable hydride (β-phase) at low pressures (<10 mbar). An additional H/(f.u.) is absorbed and reversibly desorbed at hydrogen pressures >10 mbar. The alloys and their hydriding characteristics were analyzed by means of X-ray diffraction and pressure–concentration isotherms. The two different absorption behaviours are correlated to the occupation of 96g-positions with different surrounding atomic constitutions. © 1997 Elsevier Science S.A.

Keywords: Metal Hydrides; Laves Phases; Hydrogenation; Intermetallic Compounds

1. Introduction

Some Laves phases (cubic C15 and hexagonal C14 structure) are known to absorb almost 6 H/(f.u.), e.g., $ZrV_2H_{5.6}$ [1,2]. During the hydride formation of the AB_2-type cubic Laves phase, hydrogen occupies tetrahedral interstitial sites constituted by 2 A atoms and 2 B atoms, 1 A atom and 3 B atoms, and 4 B atoms, hereafter called 2A–2B site (in the cubic C15 structure they correspond to 96g-sites), 1A–3B (32e-sites) and 4B (8b-sites), respectively. The occupation of these sites, i.e., the storage capacity H/(f.u.), is limited through the nearest neighbor distances between two sites available for hydrogen; tetrahedra with shared faces cannot be occupied at the same time [3]. With the aim of developing new low cost systems for hydrogen storage, we made alloys containing aluminum, iron, manganese and rare earth metals. Binary phase diagrams show that $CeAl_2$ and $CeFe_2$ form the cubic C15 Laves phase, but no Ce–Mn phases exist [4]. Common activation procedures (pressures up to 100 bar and temperatures up to 400 °C) did not lead to the hydride of the intermetallic compound $CeAl_2$. During the hydrogen absorption in $CeFe_2$, an amorphous hydride is formed, which decomposes into very stable CeH_x [5] and therefore hydrogen cannot be absorbed and desorbed reversibly in this intermetallic compound. In the ternary Al–Ce–Mn phase diagram [6,7] there is no indication for the existence of a Laves phase compound. However, Dwight [8] reported that some intermetallic compounds in the system RE(T, Al)$_2$ (RE=Rare Earth, T=Fe, Mn) form the cubic C15 and the hexagonal C14 Laves phases.

In the preceeding work [9] we first presented results on the new Ce($Mn_{0.5}Al_{0.5}$)$_2$ hydride including neutron scattering experiments on deuterated Ce($Mn_{0.5}Al_{0.5}$)$_2$ samples. We found that deuterium/hydrogen atoms only occupy 96g-sites and that Mn and Al atoms are randomly distributed on the 16d-sites of this cubic C15 Laves phase compound. We expanded our work on these new hydrides to other components and compositions of the intermetallic compound and show in the present work the hydriding properties of Ce($T_{1-y}Al_y$)$_2$ for $0.5 \leq y < 1.0$ and T=Fe, Mn. A model is given to explain the correlation between the measured capacities H/(f.u.) and the atomic constitutions of the tetrahedra forming the 96g-sites. The alloying and hydriding properties of Ce(T, Al)$_2$ are compared for T=Fe

*Corresponding author.

0925-8388/97/$17.00
PII S0925-8388(97)00133-3

and Mn, regarding a possible application as a low cost hydrogen storage system.

2. Experiments

All samples were prepared using high purity metals: Ce (99.9%, from Chemical Research), Mn (99.99%, from Johnson Matthey), Fe (99.99%, from Johnson Matthey) and Al (99.99%, from Alusuisse). The metals were molten in a r.f.-levitation furnace under a reduced Ar atmosphere of 0.5 bar. To improve homogeneity, the samples were re-melted three times, each time the pellet was turned up side down. Some of the samples were annealed at different temperatures and times.

X-ray diffraction was performed with a SIEMENS D500 MP Diffractometer using CuKα radiation. Lattice parameters before and after hydriding were determined from the patterns. Powders were prepared by mechanical grinding in an Ar glove box. As the compounds in powder form are pyrophoric, the powder samples for X-ray diffraction measurements were slowly poisoned by careful exposure to air.

In order to have clean surfaces for activation, large sample pieces were crushed and loaded into stainless steel autoclaves in an Ar glove box before exposing them to hydrogen gas. For the absorption measurements, we used a constant hydrogen-gas flow system (constant flow-rate of 2.0 nccm/min) and a Sievert's apparatus. Both gave the same results for samples with good absorption kinetics. For samples with poor kinetics the Sievert's apparatus was preferred (step-by-step measurement).

3. Results

The X-ray diffraction patterns of $Ce(Mn_{1-y}Al_y)_2$ with $0.5 \leq y < 1.0$ clearly show the dominant presence of the cubic C15 Laves phase structure (Fig. 1b and 1c). No annealing process was applied to these samples. It is obvious from the diffraction pattern that nearly single phase alloys were formed. Minor phases are present through very weak intensity contributions and they are

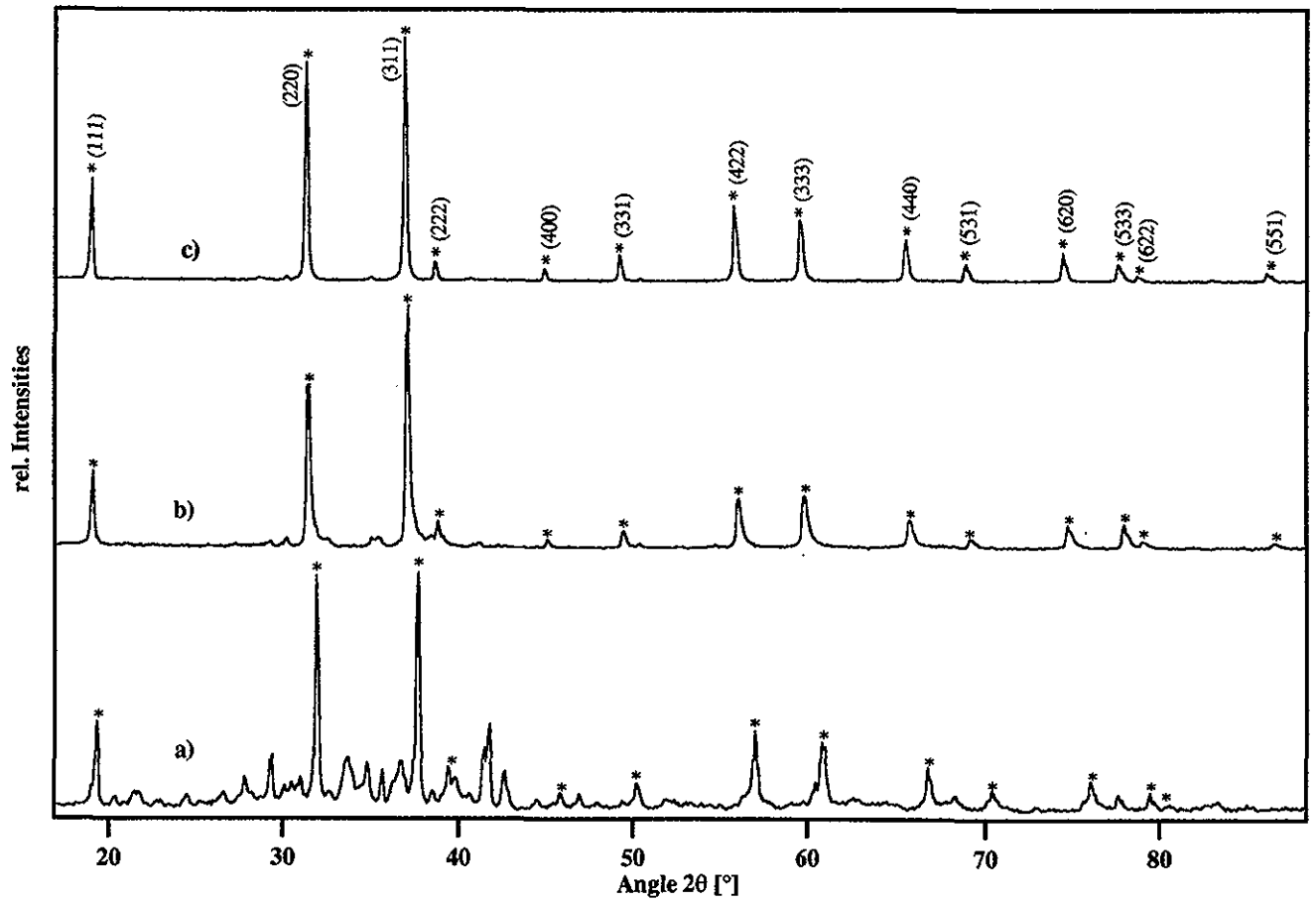

Fig. 1. The X-ray diffraction patterns of $Ce(T_{1-y}Al_y)_2$: (a) $Ce(Fe_{0.5}Al_{0.5})_2$, annealed at 900 °C for 6 days; (b) $Ce(Mn_{0.5}Al_{0.5})_2$ and (c) $Ce(Mn_{0.25}Al_{0.75})_2$ (not annealed). Lines which belong to the cubic C15 Laves phase are marked by an asterisk and the Miller indices are given. Relative intensities are represented.

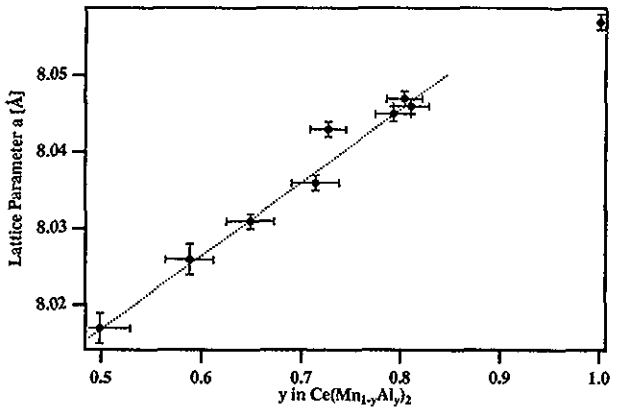

Fig. 2. Lattice parameter a (Å) vs. the Al concentration y in $Ce(Mn_{1-y}Al_y)_2$.

identified mostly as CeO impurity and Ce_2Mn_3Al (hexagonal C14 Laves phase). The lattice parameter of the main cubic Laves phase increases linearly with increasing Al concentration (Fig. 2), from $a=8.017(2)$ Å for $Ce(Mn_{0.5}Al_{0.5})_2$ to $a=8.057(1)$ Å for $CeAl_2$ (following Vegard's law). The linearity in the investigated range $0.5 \leq y < 1.0$ is a geometrical effect due to the substitution of Mn atoms with the larger Al atoms on the 16d-sites (no exchanges of atoms on the 8b-sites with atoms on the 16d-sites).

The X-ray pattern of a partially dehydrided sample clearly show shifted Bragg-reflections of the β-phase in respect to the α-phase (Fig. 3). The expansion of the unit cell ($\Delta V/V=8.9$ vol.%) is due to the incorporation of hydrogen into tetrahedral interstitial sites. No structure transformation and phase decomposition occurs during the hydrogenation (new lines in the patterns of hydrided and dehydrided samples were not observed).

The X-ray pattern of $Ce(Fe_{1-y}Al_y)_2$ alloys were similar to those of $Ce(Mn_{1-y}Al_y)_2$ (Fig. 1a). For $Ce(Fe_{1-y}Al_y)_2$, the cubic Laves phase was present in all samples with $0.5 \leq y < 1.0$. However, iron containing samples show considerable amounts of impurity phases. Four samples of $Ce(Fe_{0.5}Al_{0.5})_2$ were annealed at temperatures of 800 °C, 900 °C, 1000 °C and 1100 °C for several days. The smallest impurity phase contribution in the X-ray diffraction patterns was observed for the annealing temperature $T=$ 900 °C. However, the mass fraction of phases other than the cubic Laves phase is still too high and the portion of the absorbed quantity of hydrogen that belongs to the Laves phase cannot be determined exactly. From a semi-quantitative elemental analysis performed with electron-dispersive X-ray (EDX) we found that these alloys also contain Ce-rich phases that probably absorb hydrogen to

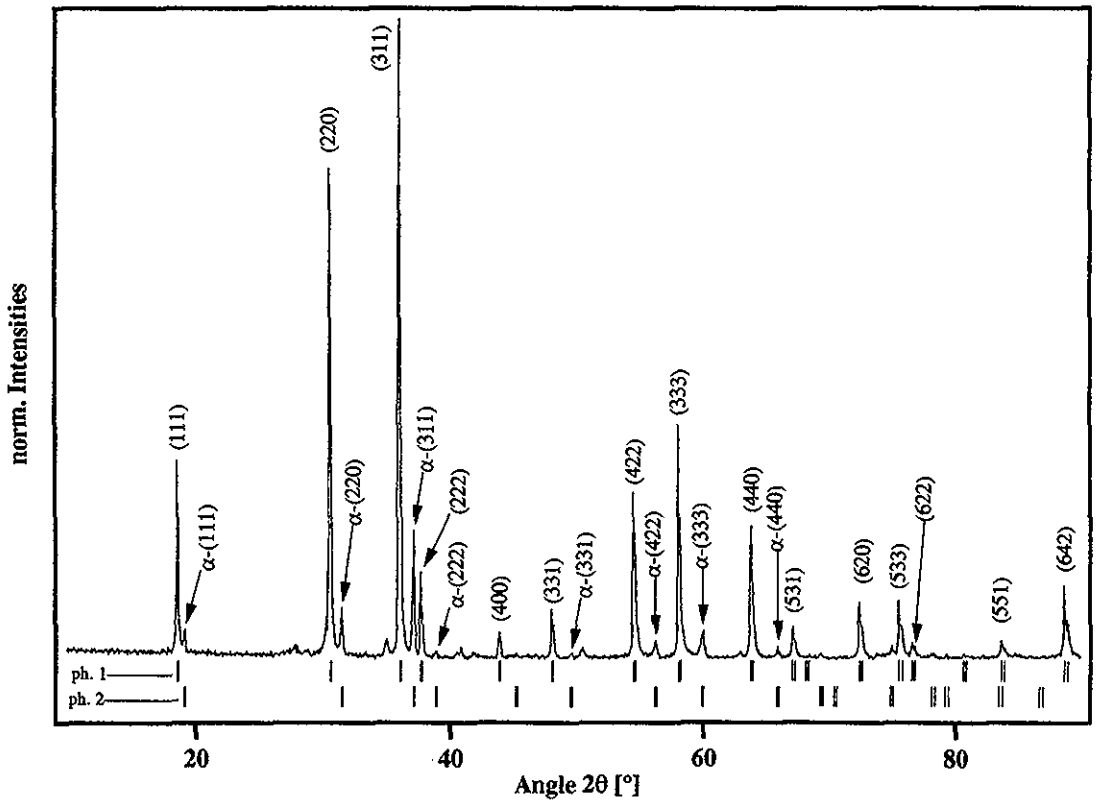

Fig. 3. X-ray diffraction pattern of $Ce(Mn_{0.5}Al_{0.5})_2H_x$ (C15 structure) at atmospheric pressure. The partially dehydrided sample shows the coexistence of two phases: ph. 1: β-phase and ph. 2: (α-phase); with the lattice parameters $a_\beta=8.242(1)$ Å and $a_\alpha=8.010(2)$ Å, respectively.

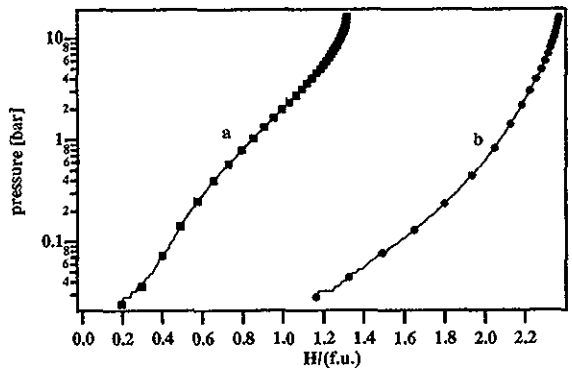

Fig. 4. Pressure–concentration isotherms for H-absorption at $T=295$ K and in the pressure range 25 mbar$<p<$15 bar for (a) $Ce(Mn_{0.25}Al_{0.75})_2$ and (b) $Ce(Mn_{0.5}Al_{0.5})_2$. The lower measurable pressure limit was 25 mbar.

form stable hydrides. Consequently, for high Fe concentrations the $Ce(Fe_{1-y}Al_y)_2$ alloys crystallize partially in the cubic Laves phase and they show multiphase behaviour. For Ce(T, Al)$_2$ with T=Fe and Mn, samples with high Al/T-ratios show smaller contributions of impurity phases. Note that for T=Mn, only small quantities of impurity phases were present even on non-annealed alloys.

We now present the results from the absorption measurements. Also these experiments show that the intermetallic compounds Ce(T, Al)$_2$ have similar properties for T=Fe and Mn. Fig. 4 shows that a fraction H/(f.u.) of the totally stored hydrogen is absorbed at low pressures and, therefore, is attributed to the formation of a stable hydride phase (β-phase), see also [9]. For T=Mn, low pressure–concentration isotherms were measured at three different temperatures: 348 K, 398 K and 448 K (Fig. 5). The equilibrium pressures at these temperatures are between 0.01 mbar and 10 mbar. Complete desorption of the β-phase could only be attained at elevated temperatures (575 K) and using a high vacuum pumping system (~10^{-6} mbar). Apart from the low pressure absorption, an additional H/(f.u.) is absorbed over a wide pressure range, from about 20 mbar to 15 bar. The strong slope in the pressure–concentration curves is unusual and mostly apparent in amorphous or disordered hydride systems and probably corresponds to the solution of further hydrogen in the β-phase without formation of a new phase. Previous results from neutron diffraction experiments on $Ce(Mn_{0.5}Al_{0.5})_2D_x$ have shown, that for $1.5<x<2.5$ the absorption is still accompanied by the occupation of 96g-sites [9]. In order to compare the hydride formation behaviour of different samples which are characterized by the slopes of the pressure–concentration curves, we calculated the derivative of the concentration H/(f.u.) by the function of the logarithm of the pressure:

$$\frac{d(H/(f.u.))}{d(\ln(p))}.$$

This consideration is related to the density of states calculation (DoS) [10] and will be a measure for the absorbed hydrogen per site energy. We applied this calculation on the absorption measurements of $Ce(Mn_{1-y}Al_y)_2$ (Fig. 6). $Ce(Mn_{0.5}Al_{0.5})_2$ has a maximum DoS at low pressure followed by a continuos decrease for higher pressures. In contrast to $Ce(Mn_{0.5}Al_{0.5})_2$, an extended DoS was observed between 1 bar and 15 bar for $Ce(Mn_{0.25}Al_{0.75})_2$. Consequently, for samples with low Mn concentration the absorption pressure curve is flattened and shows plateau-like behaviour. As the equilibrium pressure for the hydride formation is given through the Gibbs free enthalpy of formation ΔG, the width of the DoS

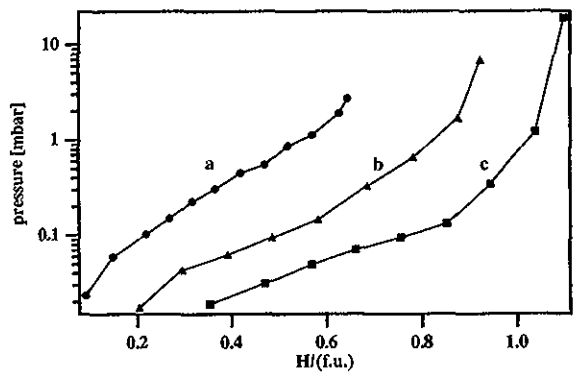

Fig. 5. Pressure–concentration isotherms for H-absorption in $Ce(Mn_{0.5}Al_{0.5})_2$ at temperatures: (a) $T=448$ K, (b) $T=398$ K and (c) $T=348$ K.

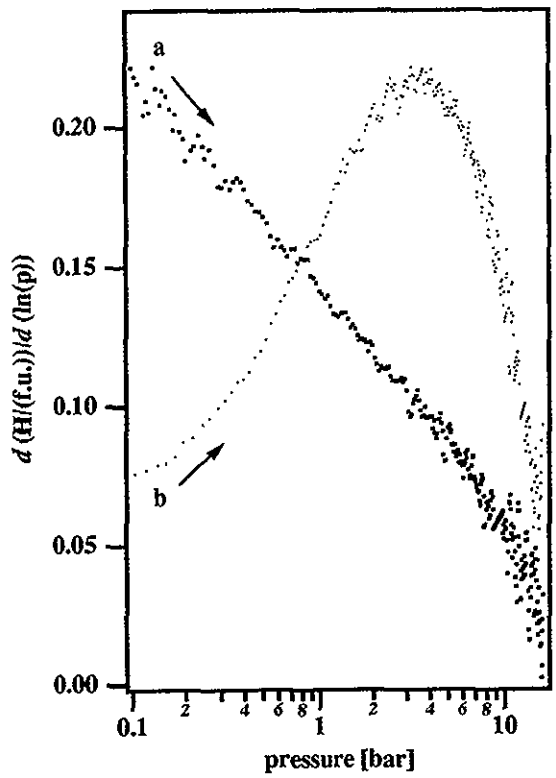

Fig. 6. Derivative of the absorbed H/(f.u.) (at $T=295$ K) in function of ln(p) for (a) $Ce(Mn_{0.5}Al_{0.5})_2$ and (b) $Ce(Mn_{0.25}Al_{0.75})_2$.

curve is attributed to the distribution of energy ΔG of the sites available for hydrogen. According to Fig. 6, the site energy disrtibution is smaller in $Ce(Mn_{0.25}Al_{0.75})_2$ than in $Ce(Mn_{0.5}Al_{0.5})_2$. A large site energy distribution is significant in a disordered system: the next neighbor arrangement and therefore the site energies vary for individual interstitials of the same type, e.g. the 96g-sites. Especially, this would be expected if Mn and Al atoms are randomly distributed on the 16d-sites in the AB_2-type Laves phase.

The two different domains in the absorption curve can be explained through the occupation of 96g-sites with different atomic constitutions, as the following considerations demonstrate. The unit cell of a cubic Laves phase with the general formula $A(B_{1-y}C_y)_2$ has 8 A-atoms and 16 B- and C-atoms. They form 96 tetrahedra surrounded by 2A–2B atoms, 2A–1B–1C atoms or 2A–2C atoms (designated as the 96g-sites). In a unit cell, the individual number of the tetrahedron type 2A–2B, 2A–1B–1C or 2A–2C, respectively, is given through the B-to-C ratio, i.e., from the stoichiometric value y. The substitution of one 16d-position affects the constitutions of 20 other tetrahedra (shared atom). In order to calculate the numbers of each tetrahedron type as a function of B–to–C ratios we labeled all 16d-positions and 96g-interstitial sites of a cluster of several unit cells. We selected a number (corresponding to y) of randomly distributed 16d-positions to be substituted with C atoms and counted the resulting number of each tetrahedron type in the cluster. It was seen that the same numbers of tetrahedra can also be obtained by calculating the probability for 2A–2B, 2A–1B–1C and 2A–2C tetrahedra by applying a binomial distribution (Fig. 7):

$$P_k = \binom{n}{k} \cdot y^k \cdot (1-y)^{n-k},$$

where n is the number of 16d-positions of the tetrahedron (equal 2 for 96g-sites); $k=0$, 1, 2 for 2A–2B, 2A–1B–1C and 2A–2C, respectively; and y the probability to replace a B-atom with a C-atom. The application of this formula is also valid for tetrahedron types 1A–3B (32e-sites) and B4 (8b-sites).

We now turn back to the absorption measurements and correlate the measured capacities to the calculated number of the 2A–2B, 2A-1B–1C and 2A–2B tetrahedron types (Fig. 8). By assuming a maximum occupation of 5 96g-positions per AB_2 formula units in the cubic Laves phase [3], we get an expected capacity for each tetrahedron type. For $Ce(Mn_{1-y}Al_y)_2$ with $0.5 \leq y < 1.0$, we found that the measured capacities in the low pressure range are in good agreement with the available number of 2Ce–2Mn tetrahedra. There is also an obvious correlation between the number of 2Ce–1Mn–1Al tetrahedra and the additional absorbed amount of hydrogen in the pressure range >10 mbar. These sites are not fully occupied as seen from Fig. 8. The ratio between the number of available 2Ce–1Mn–1Al tetrahedra and the absorbed H/(f.u.) (in the pressure range 30 mbar and 15 bar) was constant for all samples $Ce(Mn_{1-y}Aly)_2$ and its value was found to be 0.47. Consequently, only about half of the 2A–1B–1C tetrahedra are occupied in the investigated pressure range. There was no indication for the occupation of the 2Ce–2Al tetrahedra: by increasing the Al-content in $Ce(Mn_{1-y}Al_y)_2$ the total absorption capacity decreases and no absorption was observed in $CeAl_2$.

4. Conclusions

At ambient temperature and pressure conditions, the intermetallic compounds $Ce(T_{1-y}Al_y)_2$ with T=Fe, Mn form hydrides. A large fraction of the absorbed hydrogen

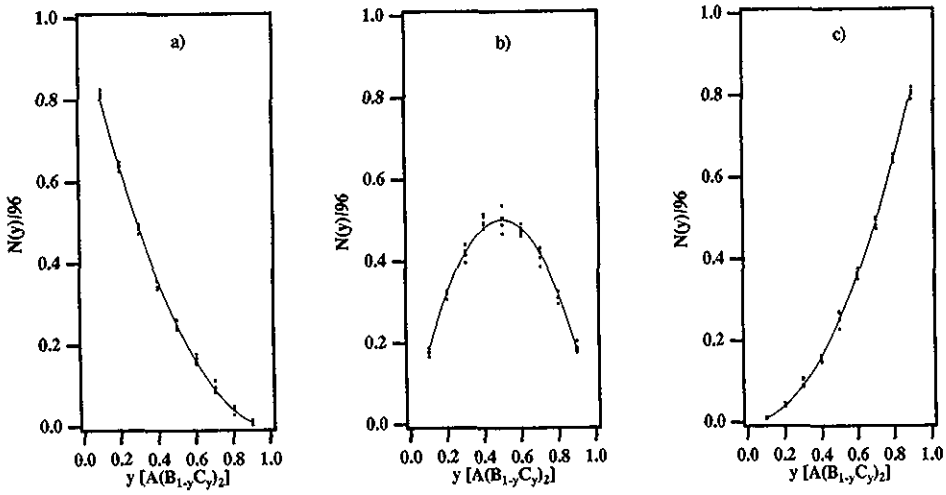

Fig. 7. Number of tetrahedra types (a) 2A–2B, (b) 2A–1B–1C and (c) 2A–2C as a function of the Al concentration y in $Ce(Mn_{1-y}Al_y)_2$. (●): values obtained from counting the tetrahedra after replacing a number of B atoms with C atoms on randomly distributed 16d-positions (for each y, the result from five sets of random distributions are represented); (———): the result of the calculation by assuming a binomial distribution of B and C atoms on the 16d-positions.

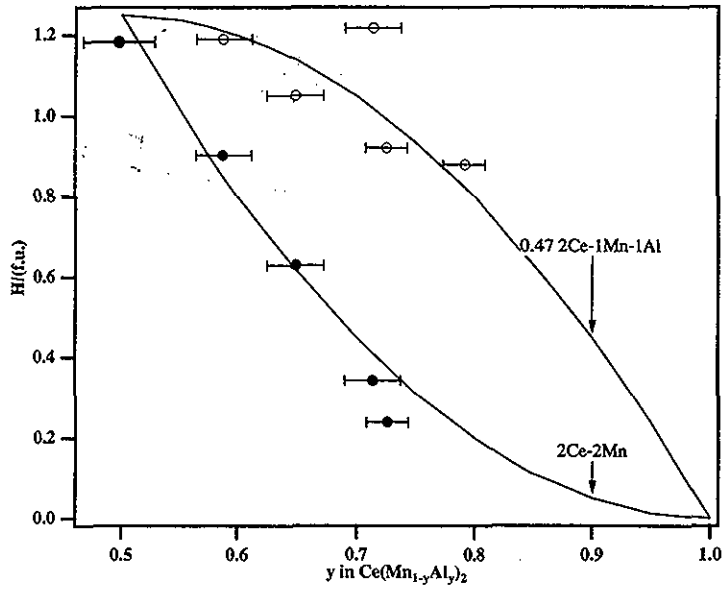

Fig. 8. Capacities H/(f.u.) as a function of the Al concentration y in $Ce(Mn_{1-y}Al_y)_2$. (———): Calculated from the model (see text). (●): Measured H/(f.u.), absorbed at low pressures (<10 mbar). (○): Measured H/(f.u.) for the reversible absorption/desorption between 25 mbar and 16 bar. Only 2A–2C and 2A–1B–1C are occupied with hydrogen.

can be reversible desorbed at ambient pressure and temperature conditions. Nearly single phase alloys of $Ce(Mn_{1-y}Al_y)_2$ are easily producible by a melting process whereas $Ce(Fe_{1-y}Al_y)_2$ alloys show strong multiphase character. Time- and energy-consuming annealing procedures may have an important influence on the production costs of such materials. The primary interest in respect to a technical application and to the development of low cost systems should be focused on the Mn containing compounds. Their storage capacity depends strongly on the Al–to–Mn ratio and decreases with increasing the Al-content. The investigated intermetallic compounds $Ce(Mn_{1-y}Al_y)_2$ have promising hydrogen storage properties in respect to a technical application. Improvements to enhance the absorption capacities are under investigation.

Acknowledgements

This work was supported by the Swiss Foundation for Energy Research (NEFF) and the Bundesamt für Energiewirtschaft (BEW).

References

[1] D. Shaltiel, J. Less-Common Met. 62 (1978) 407–416.
[2] D. Shaltiel, J. Less-Common Met. 73 (1980) 329–338.
[3] D.P. Shoemaker, C.B. Shoemaker, J. Less-Common Met. 68 (1979) 43–58.
[4] T.B. Massalski, *Binary Alloy Phase Diagrams*, ASM International, 1990.
[5] K. Aoki, T. Yamamoto, Y. Satoh, K. Fukamichi, T. Masumoto, Acta Metallica 35(10) (1987) 2465–2470.
[6] O.S. Zarechnyuk, P.I. Kripyakevich, Soviet Phys.—Crystallogr. 7(4) (1963) 436–446.
[7] O.S. Zarechnyuk, I.F. Kolobnev, M.Yu. Teslyuk, Russ. J. Inorg. Chem. 8(7) (1963) 868–870.
[8] A.E. Dwight, *Proc. Rare Earth Res. Conf., 7th*, 1968, Pub. 1969, 1, 273–282.
[9] P. Spatz, K. Gross, A. Züttel, F. Fauth, P. Fischer and L. Schlapbach, Conf. Proceedings of the Int. Symp. on Metal-Hydrogen Systems, Fundamentals and Applications, Les Diablerets, Switzerland, Aug. 25–30, 1996, J. Alloys and Comp., submitted.
[10] R. Kirchheim, W. Kieninger, X.Y. Huang, S.M. Filipek, J. Rush, T. Udovic, J. Less-Common Met. 172-174 (1991) 880.